Acoustic Scattering of Light in a Fabry-Perot Resonator

By M. G. COHEN and E. I. GORDON

(Manuscript received March 25, 1966)

Light scattering in a Fabry-Perot cavity by an acoustic beam is discussed. An heuristic treatment based on momentum conservation is used to determine the conditions, acoustic bandwidth and enhancement of the scattering interaction. A more detailed and rigorous calculation based on a coupled-mode formalism is also described. Experimental results using fused quartz Fabry-Perot cavities, single-frequency 6328Å light and acoustic waves in the frequency range 200–500 Mc/s, are presented. Enhancement relative to single-pass scattering by a factor of 50 is easily achieved. Modulation depths of twenty-five percent with a bandwidth of several megacycles have been observed.

I. INTRODUCTION

When a collimated light beam traverses a collimated high-frequency acoustic beam, it is possible for the acoustic beam to scatter light into a single, well-defined angle (into a number of well-defined angles when the acoustic frequency is sufficiently low). The amount of light scattered depends critically on the angle of the light beam relative to the acoustic wavefront (the Bragg angle) and is roughly proportional to the square of the acoustic beam width for constant acoustic intensity.[1] While it is possible to scatter all of the incident light, this usually requires impractically large amounts of acoustic power, especially at frequencies greater than a few tens of megacycles/second.

Acoustic scattering of light has considerable experimental interest since it allows a convenient method of probing transparent media to measure such things as elastic and photoelastic constants and acoustic loss or phonon lifetimes. These measurements can be made using thermally generated (Brillouin scattering)[2,3] or externally generated sound.[4] In the latter case, the scattering also allows determination of the acoustic beam shape and direction. In addition, the scattering interaction gives

rise to a class of light modulation and deflection devices.[5,6] For amplitude modulation purposes, the bandwidth of acoustic devices corresponds to the transit time of the sound across the waist of a light beam whose diffraction angle equals the diffraction angle of the sound.[5] Interest in these devices and similar ones using slow electromagnetic waves in electro-optic materials[6] would be more than academic if a sizeable percentage of the incident light could be conveniently deflected.

Resonating the acoustic medium could enhance the strength of the interaction but would excessively limit the bandwidth or transient response. On the other hand, the large velocity of light allows resonating the interaction region optically with less serious consequences to the bandwidth. Such a technique would be an extension of what has already been described for electro-optic modulation. In the Fabry-Perot electro-optic modulator,[7] the electro-optic standing wave serves to couple energy from one axial Fabry-Perot mode excited by the incident light to other axial modes. In the acoustic case, the coupling is necessarily between off-axis modes of the resonator.

Figs. 1 and 2 illustrate the arrangement required to achieve a resonant scattering interaction. For the sake of discussion, it is assumed that the incident light beam is very wide so that the angle of incidence is well defined. Under ideal conditions the sound of angular frequency Ω and velocity v travels in a plane parallel to the mirrors; unavoidably the sound travels at a very small angle Ψ relative to the mirrors as shown in Fig. 2 and this case must be considered also. The incident light of angular frequency ω and velocity c' in the medium is set at an angle θ corresponding to an off-axis resonance of the cavity. This requires that

$$k \cos \theta = a\pi/L \tag{1}$$

in which $k = \omega/c'$, L is the mirror spacing and a is an integer. Now consider Fig. 1; the scattered light with propagation constant $k' = k(1 + \Omega/\omega)$* is sent into an angle θ' defined precisely by

$$k' \sin \theta' = k \sin \theta + K \tag{2}$$

in which $K = \Omega/v$ is the acoustic propagation constant; (2) follows from the requirement of momentum conservation. The various scattered beams arising from each pass of the light will add in-phase when the angle θ' corresponds to a resonance of the cavity at the frequency $\omega + \Omega$. Hence, the angle θ' must satisfy the requirement

$$k' \cos \theta' = a'\pi/L. \tag{3}$$

* For the geometry shown, the scattered light is upshifted in frequency to a value $\omega + \Omega$. It is assumed that optical dispersion is negligible over the frequency range of interest so that $k' = (\omega + \Omega)/c'$.

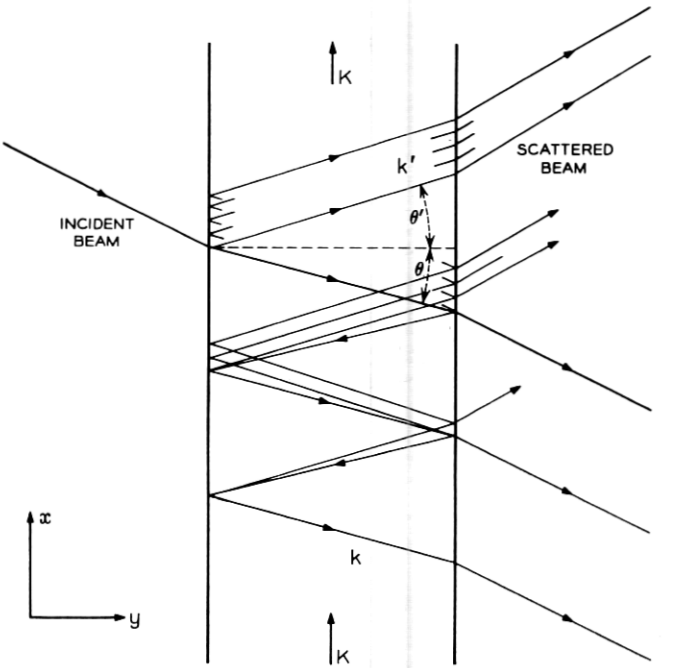

Fig. 1 — Schematic arrangement for acoustic scattering of light in an optically resonant geometry. In this case the acoustic wave travels parallel to the mirror planes.

When the acoustic beam has no y-directed momentum, momentum conservation in the y-direction (the Bragg condition) requires that

$$k' \cos \theta' = k \cos \theta \tag{4}$$

or

$$a' = a.$$

Since the acoustic beam is not extremely wide in practice, the transverse (y-directed) momentum or propagation constant is not precisely defined. This allows some deviation from the strict requirement

$$k' \cos \theta' = k \cos \theta,$$

and it is not absolutely necessary that $a' = a$. However, (4) represents the condition for optimum scattering.

Following the multiply-reflected beam, it can be seen that the Bragg condition is satisfied along each leg of the round trip, hence energy is efficiently scattered into the mode at angle θ' on each pass through the

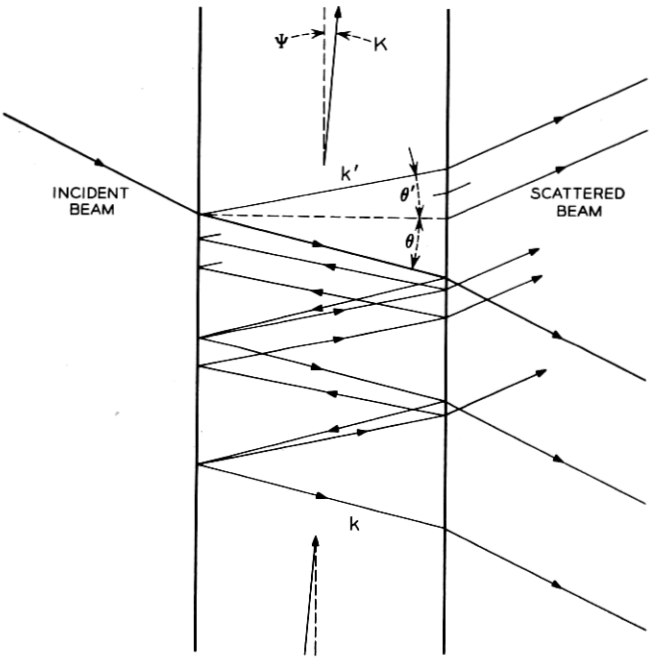

Fig. 2 — Schematic arrangement for acoustic scattering of light in an optically resonant geometry. In this case the acoustic wave travels at a small angle Ψ relative to the mirror planes.

acoustic beam. Since the effective number of passes is given approximately by $R^{\frac{1}{2}}(1 - R)^{-1}$, in which R is the mirror reflectivity,[7] the scattered optical energy is nominally increased over the single-pass value by the factor $R(1 - R)^{-2}$; for $R = 0.9$, $R(1 - R)^{-2} = 90$. The presence of loss or a finite aperture in the Fabry-Perot cavity will, of course, reduce the enhancement or gain in scattered energy.

When the acoustic beam moves at an angle Ψ as shown in Fig. 2, the situation is somewhat more complicated. The acoustic frequency must be chosen so that the angle of the scattered radiation defined by

$$k' \sin \theta' = k \sin \theta + K \cos \Psi \tag{5}$$

falls into a Fabry-Perot mode and the Bragg condition requires that

$$\begin{aligned} \pm K \sin \Psi &\approx k \cos \theta - k' \cos \theta' \\ &= (a - a')\pi/L. \end{aligned} \tag{6}$$

The requirement for $\Psi \neq 0$ can be well satisfied for either the plus or

the minus sign and hence for only one leg of the round trip as shown in Fig. 2. Thus, the enhancement of the path length is reduced by $\frac{1}{2}$ and the scattered power by $\frac{1}{4}$ over that represented by the case $\Psi \equiv 0$, (Fig. 1).

When the acoustic frequency Ω is chosen according to (5) the energy scattered from the mode excited by the incident beam will fall precisely into the optimum angle θ' for the scattered mode. When the acoustic frequency deviates from the proper value the scattering angle will vary and the scattered intensity will decrease. With the advantage of hindsight, one expects that the amount of the decrease will be determined by the angular halfwidth of the Fabry-Perot mode. For a lossless Fabry-Perot cavity the angular dependence of the transmitted intensity T is given by the Haidinger fringe formula[8] and can be written

$$T(\Omega) = \frac{1}{1 + [4R/(1 - R)^2] \sin^2 k'L [\cos \theta'(\Omega) - \cos \theta'(\Omega_o)]} \tag{7}$$

in which $\theta'(\Omega)$ and $\theta'(\Omega_o)$ are defined by (5) for different values of K (defined as Ω/v and Ω_o/v; Ω_o being the optimum acoustic frequency). Using (5), $T(\Omega)$ can be written finally as

$$T(\Omega) \approx \frac{1}{1 + [4R/(1 - R)^2] \sin^2 (\Omega - \Omega_o) (L \cos \Psi/v) \tan \theta'(\Omega_o)} \tag{8}$$

which predicts an acoustic bandwidth

$$\Delta\Omega/2\pi \approx v(1 - R)R^{-\frac{1}{2}}/2\pi L \cos \Psi \mid \tan \theta'(\Omega_o) \mid . \tag{9}$$

More detailed calculations indicate that in the limit of no loss (9) is precisely correct. An additional factor $1 + \mid \tan \theta'/\tan \theta \mid$ will appear when the angular spread of the light in the mode excited by the incident light beam of finite width is taken into account.

It may be shown by forming the product of the fraction of the incident light scattered or scattering efficiency and the bandwidth that the resonant Fabry-Perot device has a figure of merit identical to that of the nonresonant or single-pass modulation device.[9] The Fabry-Perot device has practical interest only when efficient narrow-band (<2 megacycle/second) devices are required since nonresonant modulators are difficult to optimize for narrow bandwidths.

The preceding discussion indicates in a qualitative way the properties of a scattering interaction in a Fabry-Perot cavity. In the following section, a more rigorous theory of the scattering interaction will be given which validates the simple model described above. This is followed by a description of experiments giving results in substantial agreement with the calculated results.

II. THEORY

The model chosen for discussion is that of an open Fabry-Perot cavity with unlimited x-dimension as shown in Fig. 3. The light beam is incident at an angle θ_a, at a frequency ω_a corresponding to a cavity resonance defined by

$$k_a \cos \theta_a = a\pi/L \tag{10}$$

in which $k_a = \omega_a/c'$. The cavity electric field has the form

$$\mathbf{E}(x,y,t) = \hat{k}[\exp + \alpha_a x][\exp i(\omega_a t + k_a \sin \theta_a x)] \sin (a\pi y/L) \tag{11}$$

corresponding to a decaying wave traveling to $x = -\infty$. The field is resonant in the y-dimension. The exponential loss, with loss parameter α_a, arises from the mirror reflection loss as well as internal losses in the resonator. It is shown in Appendix A that α_a is given by

$$\alpha_a = \tfrac{1}{2}k_a/Q_{L,a} \mid \sin \theta_a \mid \tag{12}$$

in which $Q_{L,a}$ is the loaded Q of the cavity (defined later). The E field is assumed to be polarized in the z-direction (denoted by $\hat{k}$).

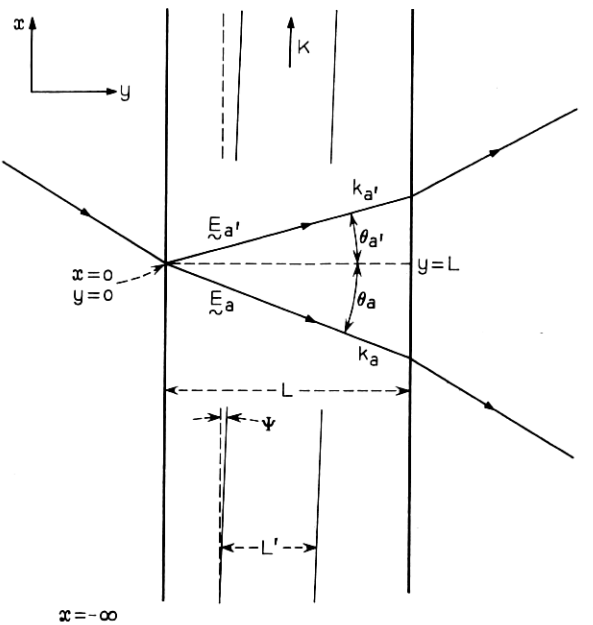

Fig. 3 — Scattering interaction geometry for coupled-mode calculation.

The eigenfunctions for the cavity, normalized in the half space $-\infty \leqq x \leqq 0$, can be written

$$\mathbf{E}_a(\omega_a) = \hat{k}(4\alpha_a/L)^{\frac{1}{2}} \sin(a\pi y/L) \exp(\alpha_a + ik_a \sin\theta_a)x. \quad (13)$$

The coupled-mode equations for the Fabry-Perot resonator are given in Ref. 7, and can be written

$$\begin{aligned} &\partial^2 e_a/\partial t^2 + \omega_a{}^2 e_a + (\omega_a/Q_{L,a})\partial e_a/\partial t \\ &\qquad + \partial^2[\langle a \mid \delta\varepsilon/\varepsilon \mid a'\rangle^* e_{a'}]/\partial t^2 \\ &\qquad\qquad = -\tfrac{1}{2}(\omega_a/Q_a)\partial e(\omega_a t)/\partial t \\ &\partial^2 e_{a'}/\partial t + \omega_{a'}{}^2 e_{a'} + (\omega_{a'}/Q_{L,a'})\partial e_{a'}/\partial t \\ &\qquad + \partial^2[\langle a \mid \delta\varepsilon/\varepsilon \mid a'\rangle e_a]/\partial t^2 \\ &\qquad\qquad = 0. \end{aligned} \quad (14)$$

Here $e_a(t)$ and $e_{a'}(t)$ are the amplitudes of the incident-beam and scattered-beam modes. The total field is given by

$$\mathbf{E} = e_a\mathbf{E}_a + e_{a'}\mathbf{E}_{a'}.$$

Note that only two modes are coupled here; any energy scattered from mode a' into an angle different from θ_a cannot correspond to a Fabry-Perot mode. (In general, the angles of the Fabry-Perot rings increase as the square root of an integer while the acoustic scattering angles increase as an integer and momentum conservation can occur for only one angle.) The quantity Q_a is the coupling Q defined by[7]

$$\begin{aligned} Q_a &= \tfrac{1}{4}\pi a(1 + R^{\frac{1}{2}})^2/(1 - R)\cos^2\theta_a \\ &\approx \pi a R^{\frac{1}{2}}/(1 - R)\cos^2\theta_a\dagger \end{aligned} \quad (15)$$

and $Q_{L,a}$ is the loaded Q defined by[7]

$$Q_{L,a}{}^{-1} = Q_a{}^{-1} + Q_d{}^{-1} \quad (16)$$

in which Q_d is the dielectric Q of the optical medium. The coupling of the Fabry-Perot modes is defined by the integral

$$\langle a \mid \delta\varepsilon/\varepsilon \mid a' \rangle = \int_{-\infty}^{0} dx \int_0^L dy\, \mathbf{E}_a \cdot [\delta\varepsilon(x,y,t)/\varepsilon]\mathbf{E}_{a'}{}^* \quad (17)$$

† The definition of Q_a given here differs from that of Ref. 7 in the appearance of the term $\cos^2\theta_a$ which has the value unity for the modes considered there. The reason for this term can be understood simply by noting that $\pi a/\cos^2\theta_a = k_a L/\cos\theta_a$ and $L/\cos\theta_a$ is the increased length over which energy is stored for the same reflection loss. Thus, the Q must be enhanced by this factor. It is also assumed that $1 + R^{\frac{1}{2}} \approx 2R^{\frac{1}{2}}$ which neglects terms of order $(1 - R)^2 \ll 1$.

in which ε is the unperturbed dielectric constant of the medium and $\delta\varepsilon$ is the perturbation produced by the sound. This can be written

$$\delta\varepsilon(x,y,t) = \delta\varepsilon \cos(\Omega t - Kx \cos\Psi - Ky \sin\Psi) \tag{18}$$

and can be written as a scalar quantity because of the choice of polarization axis. The acoustic beam travels at an angle Ψ relative to the mirrors, has a width L' and does not necessarily fill the space between mirrors. This introduces a filling factor L'/L into the expression for the coupling factor. The limits on the integration with respect to y in (17) will be taken as

$$\tfrac{1}{2}(L - L') \leqq y \leqq \tfrac{1}{2}(L + L').$$

Performing the integration, using (13) and (18) yields

$$\langle a \mid \delta\varepsilon/\varepsilon \mid a' \rangle = \tfrac{1}{2}\chi_{a,a'}(\Omega) \exp i\Omega t \tag{19}$$

with the coupling parameter $\chi_{a,a'}$ defined by

$$\chi_{a,a'}(\Omega) = \tfrac{1}{2}(\delta\varepsilon/\varepsilon)(L'/L)(i^{a-a'} \exp -i\tfrac{1}{2}(\Omega/v)L' \sin\Psi) \times \left[\frac{\sin Y_+}{Y_+} + \frac{\sin Y_-}{Y_-}\right]\left[\frac{2\alpha_a^{\frac{1}{2}}\alpha_{a'}^{\frac{1}{2}}}{\alpha_a + \alpha_{a'}}\right] \Big/ [1 + iX]. \tag{20}$$

The parameter $Y_\pm$ is given by

$$Y_\pm = \tfrac{1}{2}[(a - a')\pi \pm (\Omega/v)L \sin\Psi]L'/L. \tag{21}$$

It can be shown that $\sin Y/Y$ is precisely the frequency dependence found for single-pass scattering when the angle of the incident light is held fixed. Hence, the requirement of small Y is nothing but the condition that the angle of incidence be close to the Bragg angle.[4] Note that when $a \neq a'$ and $(\Omega/v)L \sin\Psi \approx (a - a')\pi$ so that Y_+ is small and $\sin Y_+/Y_+ \approx 1$, then $Y_- \approx (a - a')\pi$ and $\sin Y_-/Y_- \approx 0$. This corresponds to the situation described earlier (Fig. 2) in which only one leg of the round trip scatters efficiently. However, when $a = a'$ then $Y_+ = -Y_- = KL' \sin\Psi$ which can be very small only when $\Psi \to 0$. In this case, $\sin Y_+/Y_+ + \sin Y_-/Y_- = 2$ corresponding to the condition of Fig. 1 wherein both legs of the round trip scatter efficiently.

Continuing the discussion of (20) the parameter X is given by

$$X = (k_a \mid \sin\theta_a \mid + k_{a'} \mid \sin\theta_{a'} \mid - K \cos\Psi)/(\alpha_a + \alpha_{a'}) \tag{22}$$

and is zero for some acoustic frequency $\Omega_{a,a'}$ defined implicitly by

$$k_a \mid \sin\theta_a \mid + k_a(1 + \Omega_{a,a'}/\omega_a) \mid \sin\theta_{a'} \mid - (\Omega_{a,a'}/v)\cos\Psi = 0 \tag{23}$$

subject to the constraint

$$k_a \cos \theta_a = a\pi/L$$

$$k_a (1 + \Omega_{a,a'}/\omega_a) \cos \theta_{a'} = a'\pi/L.$$

It follows that

$$\Omega_{a,a'} = \frac{[k_a v/\cos \psi][|\sin \theta_a| + |\sin \theta_{a'}|]}{[1 - (v/c') \sin \theta_{a'}/\cos \Psi]} \tag{24}$$

in which θ_a and $\theta_{a'}$ are the appropriate ring angles of the Fabry-Perot cavity.† The denominator in (24) is properly set equal to unity since (v/c') sin $\theta_{a'} \sim \Omega_{a,a'}/\omega_a \ll 1$. Thus, $\Omega_{a,a'}$ represents the set of acoustic frequencies for which the scattered light will fall into a Fabry-Perot mode. There is one value of $\Omega_{a,a'}$ only for each pair of values a and a'. The parameter X may now be rewritten

$$X = 2(\Omega_{a,a'} - \Omega)[1 + (v/c') \sin \theta_{a'}/\cos \Psi]\tau_{a,a'} \tag{25}$$

$$\approx 2(\Omega_{a,a'} - \Omega)\tau_{a,a'}$$

in which

$$\tau_{a,a'} = \tfrac{1}{2}(\cos \Psi)/v(\alpha_a + \alpha_{a'}) \tag{26}$$

corresponds to a transit time of the sound across an equivalent distance $\frac{1}{2}(\alpha_a + \alpha_{a'})^{-1}$, which is related to the decay distance of the light intensity in the cavity modes. The second term in the square bracket of (25) is neglected as discussed above. Using (10), (12), and (15), $\tau_{a,a'}$ can be written finally as

$$\tau_{a,a'} = \left(\frac{\cos \Psi}{v}\right)\left(\frac{L \tan |\theta_a|}{(1 - R)R^{-\frac{1}{2}}}\right)\left[\frac{Q_a}{Q_{L,a}} + \frac{Q_{a'}}{Q_{L,a'}} \frac{\tan |\theta_a|}{\tan |\theta_{a'}|}\right]^{-1}. \tag{27}$$

The scattered amplitude can now be found by solving (14). Writing the mode amplitudes as

$$e_a = \hat{e}_a \exp i\omega_a t$$

$$e_{a'} = \hat{e}_{a'} \exp i(\omega_a + \Omega)t$$

and substituting into (14) yields

$$\hat{e}_{a'} = \frac{-\frac{1}{2}i\chi_{a,a'}Q_{L,a'}\hat{e}_a}{1 - i2(\Omega - \Omega_{a,a'})Q_{L,a'}/\omega_a}$$

$$\hat{e}_a = \frac{-\frac{1}{2}(Q_{L,a}/Q_a)e}{1 + \frac{1}{4}|\chi_{a,a'}|^2 Q_{L,a}Q_{L,a'}/(1 - i2(\Omega - \Omega_{a,a'})Q_{L,a'}/\omega_a)}. \tag{28}$$

† $|\theta_{a'}|_{\omega_a \pm \Omega_{a,a'}}$ corresponding to a ring angle for an optical frequency $\omega_a \pm \Omega_{a,a'}$ can be related to the ring angle for frequency ω_a by the formula

$$|\sin \theta_{a'}|_{\omega_a \pm \Omega_{a,a'}} \approx |\sin \theta_{a'}|_{\omega_a}[1 \pm (\Omega_{a,a'}/\omega_a) \cot^2 \theta_{a'}|_{\omega_a}].$$

Since $2Q_{L,a}/\omega_a$ is very small compared to $\tau_{a,a'}$ (the ratio is of order $(v/c')/\sin\theta_a$), the variation of $\hat{e}_a$ and $\hat{e}_{a'}$ with frequency arises almost entirely from the variation of $\chi_{a,a'}$ with frequency. Thus, the term $2(\Omega - \Omega_{a,a'})Q_{L,a'}/\omega_a$ will always be small compared to 1 in the frequency range of interest. The relative transmitted intensities in the incident and scattered modes are given by

$$\begin{aligned} T_a/T_{ao} &= [1 + \tfrac{1}{4} \mid \chi_{a,a'} \mid^2 Q_{L,a}Q_{L,a'}]^{-2} \\ T_{a'}/T_{ao} &= \tfrac{1}{4} \mid \chi_{a,a'} \mid^2 Q_{L,a'}{}^2/[1 + \tfrac{1}{4} \mid \chi_{a,a'} \mid^2 Q_{L,a}Q_{L,a'}]^2 \end{aligned} \tag{29}$$

in which T_{ao} is the transmission factor of the ath mode for $\chi_{a,a'} = 0$,

$$T_{ao} = (Q_{L,a}/Q_a)^2. \tag{30}$$

The relative scattered intensity in the absence of mirrors (single-pass) is given by[4]

$$\tfrac{1}{4}(\delta\varepsilon/\varepsilon)^2(k_aL')^2/\cos^2\theta_a\,, \tag{31}$$

while with the mirrors it is given by (for small $\chi_{a,a'}$)

$$\tfrac{1}{4} \mid \chi_{a,a'} \mid^2 Q_{L,a'}{}^2T_{ao}\,. \tag{32}$$

Under optimum conditions,

$$\mid \chi_{a,a'} \mid = (\delta\varepsilon/\varepsilon)(L'/L)2\alpha_a{}^{\frac{1}{2}}\alpha_{a'}{}^{\frac{1}{2}}/(\alpha_a + \alpha_{a'})$$

so that the optimum gain or enhancement in scattered power over that obtained in single-pass scattering can be written using (12),

$$\begin{aligned} g_{\text{opt}} = 4\frac{T_{a'o}T_{ao}}{R^{-1}(1-R)^2}\Bigg[&\left(\frac{Q_{L,a}}{Q_{L,a'}}\frac{\sin\mid\theta_a\mid}{\sin\mid\theta_{a'}\mid}\right)^{\frac{1}{2}} \\ &+ \left(\frac{Q_{L,a'}}{Q_{L,a}}\frac{\sin\mid\theta_{a'}\mid}{\sin\mid\theta_a\mid}\right)^{\frac{1}{2}}\Bigg]^{-2}. \end{aligned} \tag{33}$$

Note that for the case $a = a'$, neglecting transmission loss, $g_{\text{opt}} = R/(1-R)^2$ as expected. Under less than optimum conditions

$$\begin{aligned} g(\Omega) = g_{\text{opt}}\frac{1}{4}\Bigg[&\frac{\sin\tfrac{1}{2}[(a-a')\pi + (\Omega/v)L\sin\Psi]L'/L}{\tfrac{1}{2}[(a-a')\pi + (\Omega/v)L\sin\Psi]L'/L} \\ &+ \frac{\sin\tfrac{1}{2}[(a-a')\pi - (\Omega/v)L\sin\Psi]L'/L}{\tfrac{1}{2}[(a-a')\pi - (\Omega/v)L\sin\Psi]L'/L}\Bigg]^2 \\ &\times \frac{1}{1 + [2(\Omega - \Omega_{a,a'})\tau_{a,a'}]^2} \end{aligned} \tag{34}$$

with $\tau_{a,a'}$ given by (27). A typical curve of $g(\Omega)$ is given in Fig. 4. For

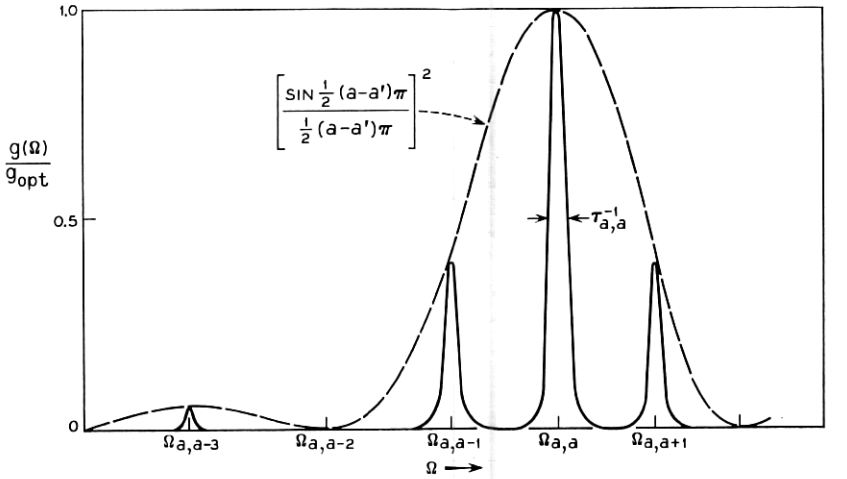

Fig. 4 — A plot of $g(\Omega)$, the enhancement factor, as a function of frequency, for the condition $\Psi = 0$ and $L = L'$.

this figure it has been assumed that $\Psi = 0$ and $L = L'$, so that

$$g(\Omega) = g_{\text{opt}} \frac{[\sin \tfrac{1}{2}(a - a')\pi/\tfrac{1}{2}(a - a')\pi]^2}{1 + [2(\Omega - \Omega_{a,a'})\tau_{a,a'}]^2}. \tag{35}$$

The maximum enhancement occurs for $a = a'$. The quantity $\tau_{a,a'}$ defined in (27) can be rewritten in terms of T_{ao} as

$$\tau_{a,a'} = \frac{\left(\frac{\cos \Psi}{v}\right)\left(\frac{L \tan |\theta_a|}{(1 - R)R^{-\frac{1}{2}}}\right) T_{ao}^{\frac{1}{2}}}{1 + (T_{ao}/T_{a'o})^{\frac{1}{2}} |\tan \theta_a/\tan \theta_{a'}|}. \tag{36}$$

The acoustic bandwidth is given by

$$\Delta\Omega/2\pi = (2\pi\tau_{a,a'})^{-1}. \tag{37}$$

The similarity to (9) is apparent.

III. EXPERIMENT

In Section II expressions were derived for the optimum frequencies for acoustic scattering, enhancement factors, and the frequency width of the scattering interaction. Experiments were performed to test the validity of these results using the apparatus depicted in Fig. 5. Light from a single-frequency 6328Å He-Ne laser (200 μ watts) was collimated by a telescope and apertured by a slit. The scattering medium or delay

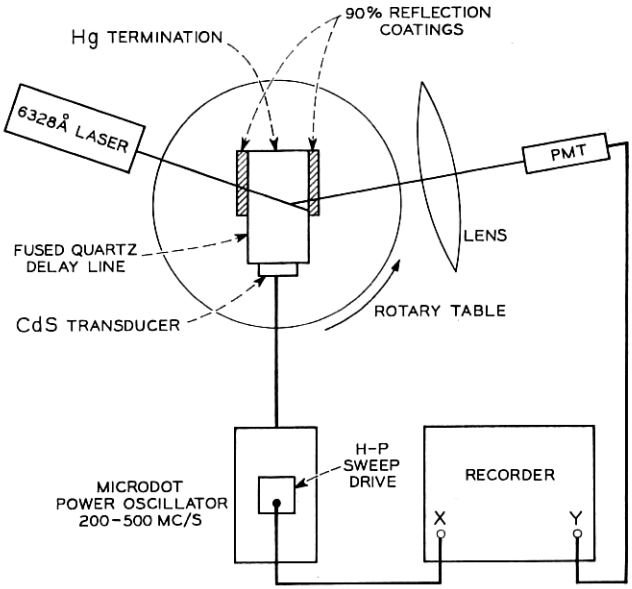

Fig. 5 — Experimental apparatus for studying acoustic scattering in a Fabry-Perot resonator.

line was fused quartz of refractive index $n = 1.457$, width $L = 1.042$ cm, and length $l = 2.5$ cm.

The Fabry-Perot cavity was formed by coating reflecting films over half the length of the delay line which was ground flat and parallel to within one fringe over its entire length. The half nearest the transducer was left without reflecting films to allow comparison of the multiple-pass scattering interaction within the Fabry-Perot cavity with single-pass scattering. The normal Fresnel reflection of the latter half was reduced by the use of quarter-wave matching films in one delay line. A second delay line had no antireflecting films.

The reflectivity of the 5-layer dielectric mirror was determined by transmission measurements to be $R = 0.89$ at 6328Å, resulting in a reflection loss pass of about 11 per cent. A value $R = 0.9$ is close to an optimum compromise between enhancement, transmission loss, and experimental convenience. The dielectric loss of the quartz was expected to be about 0.2 percent per pass yielding $Q_d \approx 50Q_a$ and $T_{ao} = (Q_{L,a}/Q_a)^2 \approx 0.96$. The measured transmission factor for normal incidence was determined to be approximately 0.80. The difference can be related to the lack of perfect parallelism in the opposing faces[10] and to the finite width

fact that the light beam was not centered perfectly in the cavity and illustrates the fact that the finite width of the mirrors resulted in walkoff for the larger ring angles. For the case shown, the on-axis mode was not resonant although it could be made resonant by warming the quartz slightly. It should be noted that the actual transmission factors taking only internal losses into account do not exhibit any variation since $\cos \theta_a \approx 1$. An analytical expression for the matching loss is given in Appendix B.

Two delay lines were studied, one with $\Psi <$ one minute of arc and the second with $\Psi \approx 14$ minutes (4×10^{-3} radians). For the first $KL \sin \Psi < \pi/3$ so that scattering could take place over both legs of the round trip. In the second case, $KL \sin \Psi \approx 4\pi$ which allowed interaction on only one leg. The acoustic transducers were evaporated CdS films with an efficiency flat to within 1 dB over the measurement range of 200–450 Mc/s. Using techniques described in Ref. 4, it was determined that the acoustic beam had an essentially uniform intensity distribution over a width of 0.7 cm. The far end of the delay line was terminated with a mercury cell with a reflection loss of 10 dB to inhibit acoustic resonances.

The scattered light was collected and focused onto a Teflon* screen on the face of the photomultiplier; the response was determined to be independent of the scattering angle in the range of interest. The output of the photomultiplier was fed into a phase-sensitive detector, the reference for which was the 1000 cycle/second square wave envelope of the modulated acoustic energy. The output of the phase sensitive detector was displayed on an X-Y recorder. The X-axis drive for the recorder was derived from an angle transducer varying the acoustic frequency. Calibration markers every one or ten megacycles/second were also generated. Absolute acoustic frequency was measured with a counter to within one kilocycle/second. Ring angles were determined to within 10 seconds of arc.

Fig. 7 illustrates typical far-field visual or photographic observations. The Fabry-Perot rings were generated by interposing a Teflon sheet and scattering the incident beam. A second exposure was taken without the Teflon sheet. The main beam was set on the first (fourth) ring and the scattered light appeared on the fourth (first) ring on the opposite side. As expected from (24) the acoustic frequency was essentially, but not exactly, the same for both cases. Closer inspection under high magnification indicated, as expected, that the ring angle for the frequency-

* Trademark of the E.I. du Pont de Nemours, Inc.

shifted, acoustically-scattered light was not quite identical to the equivalent ring angle for the light scattered by the Teflon.

Fig. 8 illustrates an experimental measurement for the case $\Psi = 14'$. The intensity of the scattered light is displayed as a function of acoustic frequency under identical conditions and fixed angle of incidence for single-pass and multiple-pass scattering. The incident beam corresponded to ring #1 and the scattered mode ring numbers are indicated above the peaks. The vertical scale for the multiple-pass scattering was larger by a factor of ten.

The enhancement factor was measured by comparing the single and multiple-pass scattered intensity. Over the frequency range shown, the single-pass scattered intensity variation with frequency was expected to show the main and one upper side lobe of a smooth $(\sin x/x)^2$ variation characteristic of Bragg scattering.[4] The distortion in frequency scale was characteristic of the oscillator frequency drive. These expectations were borne out except for the small bumps which resulted from the low Q Fabry-Perot resonances ($R = 0.035$) associated with the Fresnel reflection at the air-quartz interface. The antireflection coated delay line did not exhibit these bumps.[4] For the case $\Psi = 14'$, the measured

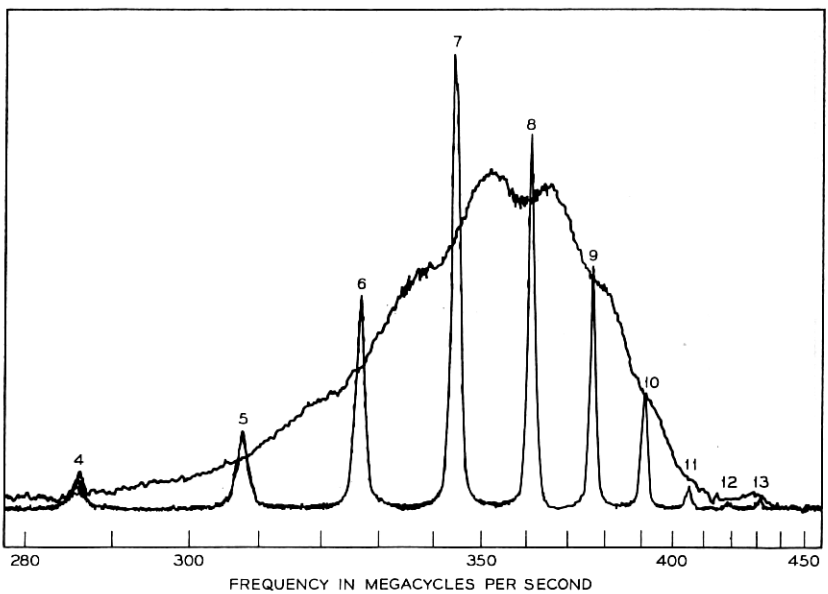

Fig. 8 — Intensity of the scattered light as a function of acoustic frequency for single-pass and multiple-pass scattering. For the latter case, the gain is reduced by a factor of 10.

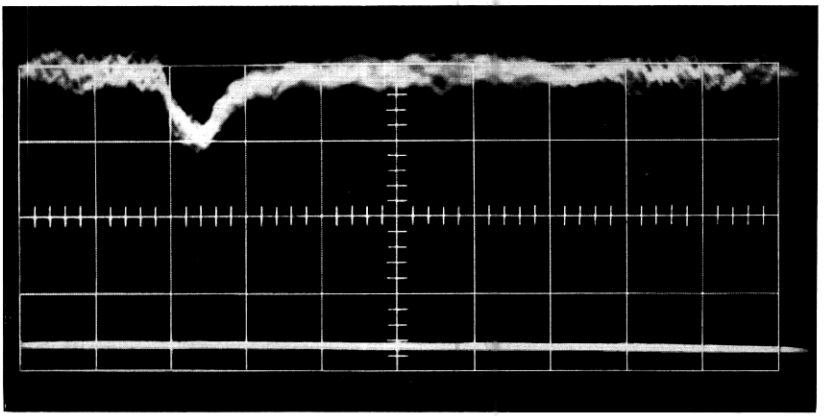

Fig. 9 — Transmitted power as a function of time. The dip corresponds to an acoustic pulse passing through the light beam which removes approximately 25 percent of the power. The acoustic frequency is 265 Mc/s and the time scale is 5 μs/cm.

Modulation depths as large as 25 percent have been observed with about 50 milliwatts of acoustic power. With efficient transducers the required microwave power could be under one watt. These parameters could be improved by the use of more efficient scattering materials than quartz.

V. ACKNOWLEDGMENT

The authors are indebted to N. F. Foster who prepared the transducers; D. L. Perry, who prepared the mirrors; J. R. Wimperis, who fabricated the delay lines, and L. B. Hooker who assisted in the experiments.

APPENDIX A

Derivation of Exponential Decay Rate of Light Within the Cavity

With respect to Fig. 10 it can be seen that when the light travels a distance ds within the cavity, the x-position is changed by an amount $dx = -|\sin \theta_a| ds$. In the absence of volume dielectric loss, the light loses energy only at the resonator surface. This loss can be approximated as a volume loss by assuming that the discrete loss upon reflection is distributed uniformly along the path of the light. This approximation is best in the limit $R \rightarrow 1$. Thus, if I represents the intensity of the

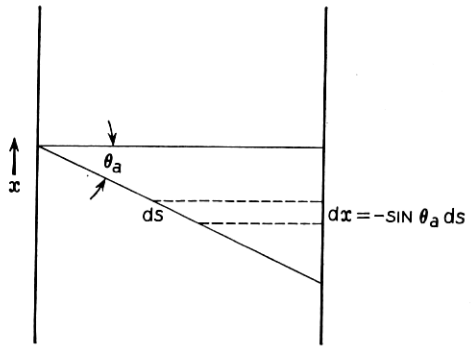

Fig. 10—Cavity geometry for deviation in appendix A.

light, the change in intensity along a path of length ds can be written

$$\begin{aligned} dI &= -I\left(\frac{k_a}{Q_d}\,ds + R^{-\frac{1}{2}}(1-R)\,\frac{\cos\theta_a\,ds}{L}\right) \\ &= +I\,\frac{k_a}{|\sin\theta_a|}\left[\frac{1}{Q_d} + \frac{R^{-\frac{1}{2}}(1-R)\cos\theta_a}{k_aL}\right]dx \end{aligned} \tag{42}$$

in which Q_d is the dielectric Q. Noting that $Q_a = k_aL/R^{-\frac{1}{2}}\,(1-R)\cos\theta_a$ and defining $Q_{L,a}^{-1} = Q_d^{-1} + Q_a^{-1}$, (42) becomes

$$\begin{aligned} dI/dx &= Ik_a/Q_{L,a}\,|\sin\theta_a| \\ &= 2\alpha_aI. \end{aligned} \tag{43}$$

The field amplitude therefore, decays as $\exp\alpha_ax$.

The validity of this result can be demonstrated by the following argument. Since the mirror surface has a phase variation given by $-k_a(\sin\theta_a)x$, the far field diffraction pattern of the light transmitted by the mirrors has the form

$$\begin{aligned} T(\theta) &= \left|\int_{-\infty}^{0}\alpha_a dx\,\exp\left[\alpha_a + ik_a\,(\sin\theta - \sin\theta_a)x\right]\right|^2 \\ &= \frac{1}{1 + [(k_a/\alpha_a)\,(\sin\theta - \sin\theta_a)]^2}. \end{aligned} \tag{44}$$

Using (43)

$$\begin{aligned} T(\theta) &= \frac{1}{1 + [2Q_{L,a}\sin\theta_a\,(\sin\theta - \sin\theta_a)]^2} \\ &\approx \frac{1}{1 + [2Q_{L,a}\cos\theta_a\,(\cos\theta - \cos\theta_a)]^2}. \end{aligned} \tag{45}$$

enhancement factors and bandwidths agreed to about 5 percent which was better than could be expected.

The most detailed measurements were made for the case $\Psi < 1'$. Verification of (24) for the frequency of the interaction was obtained by determining $\Omega_{a,a'}$ and θ_a and writing (24) as

$$v = \frac{\lambda_0(\Omega_{a,a'}/2\pi)\cos\Psi}{n[|\sin\theta_a| + |\sin\theta_{a'}|(1 \pm \Omega_{a,a'}/\omega_a)\cot^2\theta_{a'})]} \tag{38}$$

in which λ_0 is the vacuum wavelength and n the index of refraction of the quartz, and computing v from the measured frequencies and mode angles. The angles θ_a were sufficiently small (of order 10^{-2} radians) that $n \sin\theta_a$ could be taken equal to the externally measured ring angles and λ_0 to the air wavelength. The measured ring angles were consistent with those computed for the cavity. The data yielded a value $v = 5.940 \pm 0.005 \times 10^5$ cm/sec, consistent with the uncertainty in measuring θ_a. Measurements in the single-pass scattering region were also made by determining the Bragg angle Θ for scattering to $\omega \pm \Omega$ defined by

$$\sin\Theta_\pm = v/c' \mp \tfrac{1}{2}K/k' \tag{39}$$

which yields

$$\Theta_- - \Theta_+ \approx \sin\Theta_- - \sin\Theta_+ = K/k'. \tag{40}$$

The phase velocity is determined by

$$v = (\Omega/2\pi)\lambda_0/\Delta\theta \tag{41}$$

in which $\Delta\theta$ is the externally determined difference between the two Bragg angles. The phase velocity was determined by this technique to be 5.940×10^5 cm/sec with the same spread in measured values, in agreement with the optical Fabry-Perot measurements. The phase velocity was also determined by setting the incident light at the Bragg angle in the single-pass region and using the intensity of the scattered light as a measure of the acoustic intensity while the acoustic frequency was varied through a range of 2 megacycles/second. The acoustic Fabry-Perot resonances were emphasized by removing the mercury from the far end. Using the relation

$$\Delta\Omega/2\pi = v/2l$$

in which l is the length of the fused quartz bar and $\Delta\Omega/2\pi$ is the spacing of the resonances yielded a value $v = (5.950 \pm 0.003) \times 10^5$ cm/second. While the difference here is small, it falls outside the range of

experimental uncertainty. The difference has been ascribed tentatively to pulling of the acoustic resonances by the transducer. The values of v quoted in the literature[11,12] fall in the range $5.90 - 5.96 \times 10^5$ cm/second.

Comparison with theory of experimentally determined values of enhancement and bandwidth is hampered slightly by an uncertainty in the value of $(1 - R)$ which could be as large as ± 10 percent. On the other hand, the product

$$(\Delta\Omega/2\pi)g_{\text{opt}}^{\frac{1}{2}}$$

using (33), (37), and (36) is independent of R. Preliminary measurements for the case $\Psi = 14'$ were very encouraging. Since the case $\Psi < 1'$ was believed to be more interesting most of the measurements were made here. To simplify interpretation, the measurements were restricted to scattering from a given ring to the same ring on the other side of normal incidence $(a \rightarrow a)$. Some of these measurements are summarized in Table I. The calculations were performed taking $T_{ao} = 0.96$, however, correcting g_{opt} for the matching loss as experimentally determined. In all cases both $\Delta\Omega/2\pi$ and $g_{\text{opt}}^{\frac{1}{2}}$ were larger than calculated, the product being as much as 80 percent larger than expected. Values smaller than expected could possibly be attributed to an imperfect Fabry-Perot cavity. No explanation for the larger values can be offered at this time.

Under optimum conditions, the modulation depth was approximately 25 percent as shown in Fig. 9. The acoustic power was estimated to be about 50 milliwatts.

IV. CONCLUSION

Experiments illustrating acoustic scattering in a Fabry-Perot resonator have been described and compared with a coupled-mode theory. The acoustic frequencies for resonant scattering agree with theory to within the experimental uncertainty of 1:500. The agreement on enhancement factors and bandwidth is within 80 percent but well outside experimental uncertainty; the measured values are on the large side.

TABLE I

Ring	$(\Omega_{a,a}/2\pi)$ (Mc/s)	g_{ex}	$(\Delta\Omega/2\pi)_{ex}$ Mc/s)	$(g^{\frac{1}{2}}\Delta\Omega/\pi)_{ex}$ (Mc/s)	$(g^{\frac{1}{2}}\Delta\Omega/2\pi)_{calc.}$ (Mc/s)
2	220	73.3	3.1	26.5	17
3	283	47	3.27	22.5	12.5
4	333	49	1.94	13.6	10.5

Note that when there is no internal loss, $Q_{L,a} = Q_a = k_a L R^{\frac{1}{2}}/(1 - R) \cos \theta_a$ and

$$T(\theta) \approx \frac{1}{1 + [4R/(1 - R)^2][k_a L(\cos \theta - \cos \theta_a)]^2} \tag{46}$$

which corresponds very closely to the Haidinger fringe formula in the limit $R \to 1$. Thus, the approximate expression for the optical decay (43) is most valid in this limit.

It can be shown that the difference between the Lorentzian form of (46) and the true Haidinger fringe formula arises from the approximation in which the discrete reflection is replaced by a fictitious volume loss; the stepwise decay of the light intensity becomes an exponential decay. This approximation is, of course, best when the steps become vanishingly small, i.e., when $R \to 1$. A demonstration of the more precise result is straightforward but lengthy and will not be included here.

APPENDIX B

Derivation of Cavity Transmission for Off-Axis Modes

Assuming that the cavity transmission for a given mode may be approximated by $T(\theta)$ given in (46) and the energy distribution of the incident beam by $F(\theta)$ then the transmission factor may be written

$$T = \frac{\int_{-\pi/2}^{+\pi/2} F(\theta)T(\theta)d\theta}{\int_{-\pi/2}^{+\pi/2} F(\theta)d\theta}. \tag{47}$$

For an incident beam with rectangular cross section of width W incident at angle θ_a,

$$F(\theta) = \left[\frac{\sin \frac{1}{2}kW(\sin \theta - \sin \theta_a)}{\frac{1}{2}kW(\sin \theta - \sin \theta_a)}\right]^2 \tag{48}$$

and

$$T \approx \frac{\int_{-\infty}^{+\infty} [\sin^2 x/x^2(1 + a^2x^2)]dx}{\int_{-\infty}^{+\infty} [\sin^2 x/x^2]dx} \tag{49}$$

in which

$$a^2 = \frac{16R}{(1 - R)^2}\left[\frac{L \tan \theta_a}{W}\right]^2.$$

The integral in (49) can be evaluated by a straight-forward contour integration to yield

$$T = 1 - ae^{-a^{-1}} \sinh a^{-1}. \tag{50}$$

In the limit $(L \tan \theta_a/W) \propto a \to 0$, $T = 1$, as would be expected, since the angular spread in the incident beam is small compared to the angular spread of the cavity mode. In the opposite limit $(L \tan \theta_a/W) \propto a \to \infty$, $T \approx a^{-1}$ and the transmission factor for successive cavity modes of increasing angle θ_a varies as cot θ_a .

REFERENCES

1. Born, M., and Wolf, E., *Principles of Optics*, Pergamon Press, New York, 1959, Chap. XII.
2. Benedek, G. B., Lastovka, J. B., Fritsch, K., and Greytak, T., Brillouin Scattering in Liquids and Solids Using Low Power Lasers, J. Opt. Soc. Amer., *54*, October, 1964.
3. Chiao, R. Y. and Stoicheff, B. P., Brillouin Scattering in Liquids Excited by the He-Ne Maser, J. Opt. Soc. Amer., *54*, 1964, p. 1286.
4. Cohen, M. G. and Gordon, E. I., Acoustic Beam Probing Using Optical Techniques, B.S.T.J., *44*, 1965, p. 693.
5. Gordon, E. I. and Cohen, M. G., Electro-optic Diffraction Gratings for Light Beam Modulation and Diffraction, IEEE J. Quantum Elect., *1*, August, 1965
6. Cohen M. G. and Gordon, E. I., Electro-optic [$KTa_xNb_{1-x}O_3$ (KTN)] Gratings for Light Beam Modulation and Deflection, Appl. Phys. Let., *5*, 1964, p. 181.
7. Gordon, E. I. and Rigden, J. D., The Fabry-Perot Electro-optic Modulator, B.S.T.J., *42*, 1963, p. 155.
8. Jenkins, F. A. and White, H. E., *Fundamentals of Optics*, McGraw-Hill Book Company, Inc., New York, 1937, p. 87.
9. Gordon, E. I., Figure of Merit for Acousto-Optical Deflection and Modulation Devices, IEEE J. Quantum Elect., *2*, (Correspondence), May, 1966, p. 104.
10. Del Piano, V. N., Jr. and Quesada, A. F., Transmission Characteristics of Fabry-Perot Interferometers and a Related Electro-optic Modulator, Appl. Opt., *4*, November, 1965, pp. 1386–1390.
11. Mason, W. P., *Physical Acoustics and the Properties of Solids*, D. Van Nostrand Co., Inc., 1958, p. 17.
12. *Handbook of Chemistry and Physics*, Chemical Rubber Co., Cleveland, Ohio, 1964.

of the incident light beam which resulted in an angular spread comparable to or larger than the angular width of the Fabry-Perot modes. The measured transmission factors for off-axis modes were smaller than the value for the on-axis mode since the angular width decreases with increasing mode angle. This is illustrated in the photograph of Fig. 6 which displays the transmission factor of the cavity as a function of angle of the incident light relative to the surface normal. The upper line is unity transmission. The measured transmission factors became increasingly smaller for increasing mode angle indicating that as the angular spread of the rings became increasingly smaller, less of the incident light was matched into the cavity mode. This situation, while normally undesirable and easily avoidable, was experimentally convenient since it guaranteed that the dominant feature of the light distribution in the incident beam mode was an exponential decay as postulated in Section II. The incident beam mode usually corresponded to a relalatively small angle and the matching loss was not excessively large. The lack of perfect symmetry about normal incidence arose from the

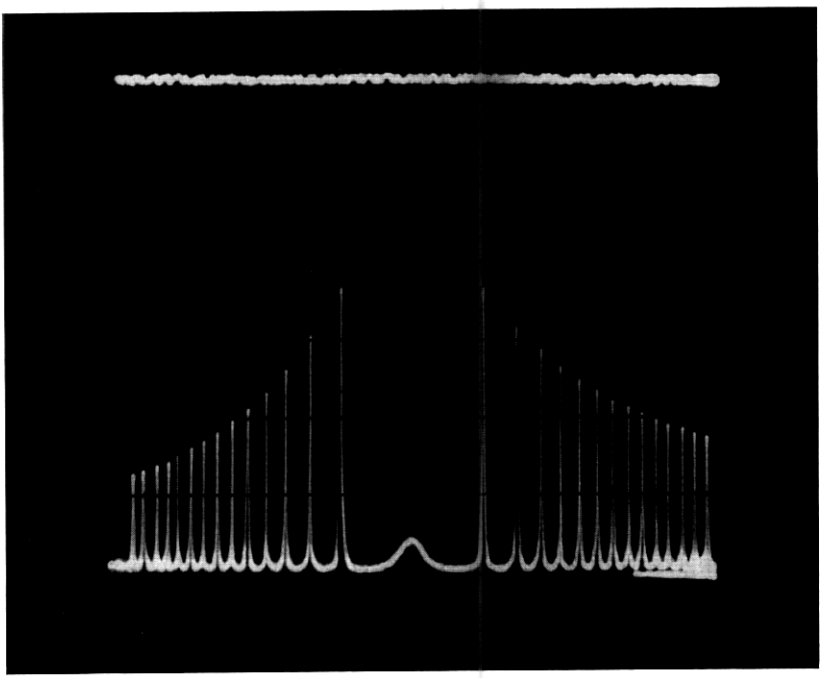

Fig. 6 — Measured Fabry-Perot cavity transmission factors as a function of angle of the incident light relative to the surface normal.

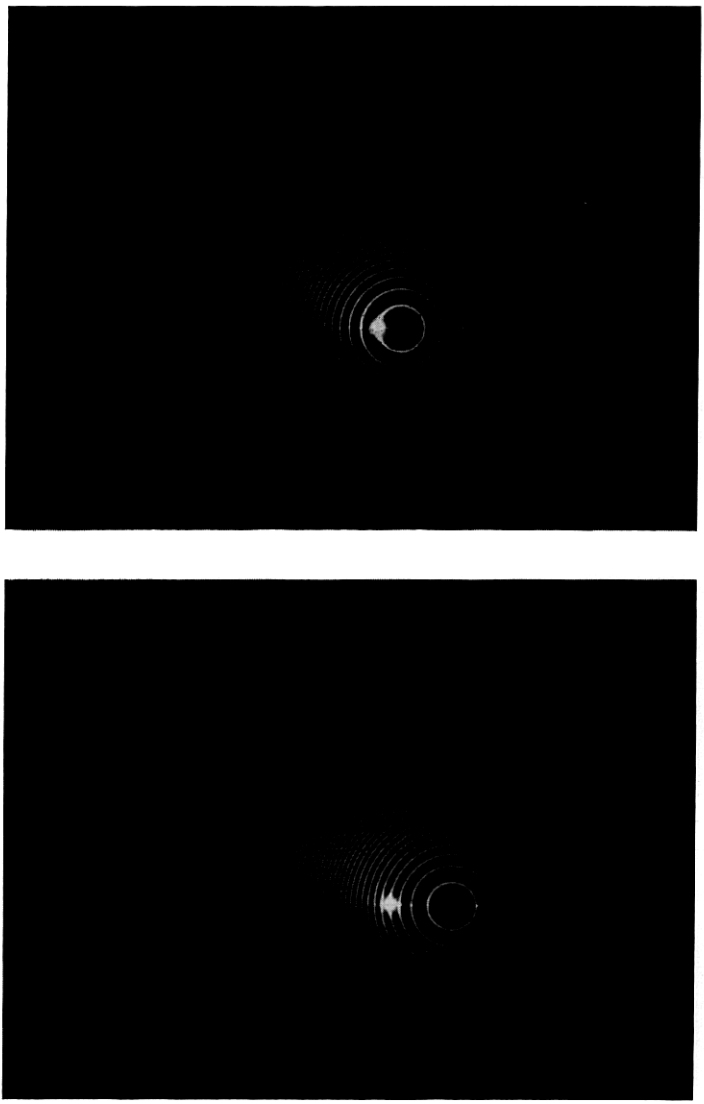

Fig. 7 — Photographs of typical far-field observations of scattering in the Fabry-Perot resonator. The angles of the incident and scattered beams are interchanged in the two photographs.